Research Article
Field-Weakening Nonlinear Control of a Separately Excited DC Motor

Mohamed Zribi and Adel Al-Zamel

This paper investigates the design and implementation of nonlinear control schemes for a separately excited DC motor operating in the field-weakening region. A feedback linearization controller, a Corless-Leitman-type controller, and two nonlinear controllers are designed and implemented for a DC motor system. The stability of the closed-loop system is proved using Lyapunov theory. A hardware testbed is constructed to experimentally verify the designed controllers. The hardware consists of a DC motor system, a DSP controller board, a power module, two current sensors, and a tachogenerator. The experimental results indicate that the developed controllers work well.

1. Introduction

Generally, DC motors are used in a huge number of industrial applications. In particular, separately excited DC motors have many applications. The operation of separately excited DC motors is as follows. Field coils are used to establish an air-gap flux between stationary iron poles and the rotating armature which has axially directed conductors that are connected to a brush commutator; these conductors are continuously switched such that those located under a pole carry similarly directed currents. The interaction of axially directed currents and radially directed field flux produces a shaft torque. DC motors and drives generally contain nonlinear relations that are difficult to model. In addition, in a number of cases, even when the available model is accurate, the exact system parameters are difficult to measure or estimate. Modern nonlinear control techniques, in conjunction with improved power electronics and fast digital signal processing tools, can be used to overcome the nonlinearity of the system and to ensure that the system behaves in the desired manner.

Many researchers have addressed the control of electrical machines and specifically the control of DC motors, for example refer to [1–10]. Several authors have tackled the control problem of electrical machines operating in the field-weakening region. For example, Briz et al. [11], Buente et al. [12], Sattler et al. [13], and Seibel et al. [14] dealt with the control of induction motors operating in the field-weakening region. Krishnan [15] explored the field-weakening control of a PM synchrounous motor and Nishikata et al. [16] proposed a field-weakening speed control system for a self-regulated synchronous motor.

Several researchers have contributed to the control of DC motors operating in the field-weakening region. Liu et al. [17–20] proposed several strategies to control a DC motor in the field-weakening region. They used the input-output feedback linearization technique, the backstepping technique combined with variable structure control, the load-adaptive and sensorless control technique, and other nonlinear control options to control the system. Matausek et al. [21] proposed an adaptive controller for a DC motor drive operating in the field-weakening region. The adaptation update law is based on gain scheduling; the theoretical result is supported by simulations and experimental results. Matausek et al. [22] also proposed the internal model control structure to regulate a DC motor drive in the field-weakening region; they used a feedforward neural network inverse model with one hidden layer and a small number of hidden neurons to control the system. Zhou et al. [23] designed a nonlinear adaptive backstepping speed controller for the field-weakening region of a separately excited DC motor; the theoretical results are verified through computer simulations. Zhou et al. [24] also designed a global speed controller for the DC motor; the authors used two models to represent the system: a linear model was used to describe the system when the motor is operating under the base speed and a nonlinear model was used to describe the system operating in the field-weakening region. A linear robust state-feedback controller was proposed to control the system under the linear model hypothesis while an adaptive backstepping control scheme is designed for the control of the nonlinear model. Simulations results were presented to test the proposed controllers. Miti and Renfrew [25] and Miti et al. [26] studied the field-weakening control problem of brushless DC motors. Zeroug et al. [27] addressed the problem of performance prediction and field-weakening simulation of a brushless DC motor.

This paper uses four nonlinear techniques to control a separately excited DC motor operating in the field-weakening region. Using Lyapunov theory, it is proved that the controllers guarantee the stability of the closed-loop system. The proposed control schemes are implemented using a developed testbed. The implementation results show the effectiveness of the proposed controllers.

The paper is organized as follows. A mathematical model for the DC motor operating in the field-weakening region is given in Section 2. A feedback linearization controller is designed in Section 3. A Corless-Leitman-type controller is proposed in Section 4. Two continuous nonlinear controllers are developed in Section 5. A description of the hardware setup is given in Section 6. The implementation results are presented and discussed in Section 7. Finally, the conclusion is given in Section 8.

2. Mathematical model of a separately excited DC motor

The equations describing a separately excited DC motor are as follows:

$$\frac{di_a}{dt} = \frac{1}{L_a}(v_a - R_a i_a - K_m i_f \omega),$$

$$\frac{di_f}{dt} = \frac{1}{L_f}(v_f - R_f i_f),$$

$$\frac{d\omega}{dt} = \frac{1}{J_m}(K_m i_a i_f - B_m \omega - T_l),$$

(2.1)

where i_a and i_f are the armature and field currents; ω is the rotor speed. The voltages v_a and v_f are the armature and field voltages. The resistances R_a and R_f are the armature and field resistances; L_a and L_f are the armature and field inductances. The constant K_m is the motor torque constant, J_m is the inertia of the motor, B_m is the damping coefficient. The load torque is T_l.

Define the following constants:

$$K_1 = -\frac{R_a}{L_a}, \qquad K_2 = -\frac{K_m}{L_a}, \qquad K_3 = -\frac{R_f}{L_f}, \qquad K_4 = \frac{K_m}{J_m}, \qquad K_5 = -\frac{B_m}{J_m}. \qquad (2.2)$$

Also, let

$$x_1 = i_a, \qquad x_2 = i_f, \qquad x_3 = \omega. \qquad (2.3)$$

Therefore, the equations describing a separately excited DC motor can be written as

$$\dot{x}_1 = K_1 x_1 + K_2 x_2 x_3 + \frac{1}{L_a} v_a,$$

$$\dot{x}_2 = K_3 x_2 + \frac{1}{L_f} v_f,$$

$$\dot{x}_3 = K_4 x_1 x_2 + K_5 x_3 - \frac{\tau_l}{J_m}.$$

(2.4)

Remark 2.1. The design of the controllers will be performed without taking the load torque into account. An observer can then be designed to estimate the load torque [28].

The design of the observer is described below.

Let $x_4 = -\tau_l/J_m$ and assume that the load is constant. Using the last equation of (2.4) and the fact that the load is constant, we have the following system:

$$\dot{x}_3 = K_4 x_1 x_2 + K_5 x_3 + x_4,$$

$$\dot{x}_4 = 0.$$

(2.5)

Let l_1 and l_2 be properly chosen positive scalars. Since x_1, x_2, and x_3 are measurable, we define the observer to be

$$\dot{\hat{x}}_3 = K_4 x_1 x_2 + K_5 x_3 + \hat{x}_4 + l_1 (x_3 - \hat{x}_3),$$

$$\dot{\hat{x}}_4 = l_2 (x_3 - \hat{x}_3). \tag{2.6}$$

Define the error e_o such that $e_o = \begin{bmatrix} e_3 & e_4 \end{bmatrix}^T = \begin{bmatrix} x_3 - \hat{x}_3 & x_4 - \hat{x}_4 \end{bmatrix}^T$. The error e_o satisfies the equation $\dot{e}_o = A_o e_o$, where

$$A_o = \begin{bmatrix} -l_1 & 1 \\ -l_2 & 0 \end{bmatrix}. \tag{2.7}$$

Since l_1 and l_2 are chosen to be positive, then the error $e_o(t)$ converges to zero asymptotically. Hence, the above observer can be used to estimate $x_4 = -\tau_l / J_m$.

Next, we use a mathematical transformation to write the model of the system into a form that facilitate the design of control schemes. Consider the following change of variables:

$$\zeta_1 = x_3,$$

$$\zeta_2 = K_4 x_1 x_2 + K_5 x_3, \tag{2.8}$$

$$\zeta_3 = x_2.$$

For $\zeta_3 \neq 0$, the inverse of the transformation given in (2.8) is such:

$$x_1 = \frac{1}{K_4 \zeta_3} (\zeta_2 - K_5 \zeta_1),$$

$$x_2 = \zeta_3, \tag{2.9}$$

$$x_3 = \zeta_1.$$

Define the new inputs u_1 and u_2 such that

$$\begin{bmatrix} u_1 \\ u_2 \end{bmatrix} = \begin{bmatrix} \dfrac{K_4}{L_a} x_2 & \dfrac{K_4}{L_f} x_1 \\ 0 & \dfrac{1}{L_f} \end{bmatrix} \begin{bmatrix} v_a \\ v_f \end{bmatrix}. \tag{2.10}$$

Therefore, the equations of the separately excited DC motor can be written as functions of the new variables ζ_1, ζ_2, ζ_3, and the new inputs u_1, u_2 such that

$$\dot{\zeta}_1 = \zeta_2,$$

$$\dot{\zeta}_2 = -(K_1 K_5 + K_3 K_5)\zeta_1 + (K_1 + K_3 + K_5)\zeta_2 + K_2 K_4 \zeta_1 \zeta_3^2 + u_1, \tag{2.11}$$

$$\dot{\zeta}_3 = K_3 \zeta_3 + u_2.$$

The equations given in (2.11) can be written in compact form as

$$\dot{\zeta} = A\zeta + Bf + Bu, \tag{2.12}$$

where

$$A = \begin{bmatrix} 0 & 1 & 0 \\ -(K_1 + K_3)K_5 & K_1 + K_3 + K_5 & 0 \\ 0 & 0 & K_3 \end{bmatrix}, \qquad \zeta = \begin{bmatrix} \zeta_1 \\ \zeta_2 \\ \zeta_3 \end{bmatrix},$$

$$B = \begin{bmatrix} 0 & 0 \\ 1 & 0 \\ 0 & 1 \end{bmatrix}, \qquad f = \begin{bmatrix} K_2 K_4 \zeta_1 \zeta_3^2 \\ 0 \end{bmatrix}, \qquad u = \begin{bmatrix} u_1 \\ u_2 \end{bmatrix}. \tag{2.13}$$

Remark 2.2. It is assumed that the nonlinear term f is bounded by a known function η such that

$$\|f\| = K_2 K_4 \zeta_1 \zeta_3^2 \leq \eta. \tag{2.14}$$

This assumption is reasonable because it is always possible to find η such that, $\eta \geq K_2 K_4$ $\omega_{\max} i_{f\,\max}^2$, where $\omega_{\max}$ corresponds to the maximum value of ω and $i_{f\,\max}$ corresponds to the maximum value of i_f.

Let the matrix A_c be such that

$$A_c = A - BK, \tag{2.15}$$

where the gain K is selected such that the matrix $A_c = A - BK$ is a stable matrix.

The next four sections deal with the design of nonlinear controllers for the DC motor system. The objective of the controllers is to regulate the speed of the motor to a desired constant value. Note that the desired speed is chosen above the rated speed of the motor.

The following variables are needed for the design of the controllers. Let ζ_d be the desired value of ζ such that

$$\zeta_d = \begin{bmatrix} \zeta_{1d} \\ \zeta_{2d} \\ \zeta_{3d} \end{bmatrix} = \begin{bmatrix} \omega_d \\ 0 \\ i_{fd} \end{bmatrix}, \tag{2.16}$$

where ω_d represents the desired constant speed and i_{fd} represents the desired constant field current.

Define the error e such that

$$e = \zeta - \zeta_d. \tag{2.17}$$

Also, let the reference input of the system be $r = [r_1 \quad r_2]^T$ such that

$$A\zeta_d + Br = 0. \tag{2.18}$$

Hence, the reference input is chosen as

$$r = \begin{bmatrix} r_1 \\ r_2 \end{bmatrix} = \begin{bmatrix} \left(\dfrac{R_a}{L_a} + \dfrac{R_f}{L_f} \right) \dfrac{B}{J} \omega_d \\ \dfrac{R_f}{L_f} i_{fd} \end{bmatrix}. \tag{2.19}$$

3. A Feedback linearization controller for the DC motor

The equations of the DC motor system can be written in compact form as

$$\dot{\zeta} = A\zeta + Bf + Bu. \tag{3.1}$$

PROPOSITION 3.1. *The feedback linearization control law*

$$u = -f - Ke + r \tag{3.2}$$

when applied to the separately excited DC motor system guarantees the asymptotic convergence to zero of the errors of the system.

Proof. Using (2.17), (3.1), (3.2), (2.18), and (2.15), it follows that

$$\dot{e} = \dot{\zeta} = A\zeta + Bf + Bu = A\zeta + Bf + B(-f - Ke + r) = (A - BK)e + A\zeta_d + Br = A_c e. \tag{3.3}$$

Since the pair (A, B) is controllable, the poles of the closed-loop system can be selected such that the response of the system is as desired. Thus, if A_c is chosen to be a stable matrix, the errors are guaranteed to converge to zero asymptotically. Hence, the closed-loop system is asymptotically stable. □

4. A Corless-Leitmann-type controller for the DC motor

When designing the feedback linearization controller, it was assumed that the nonlinearities of the system can be canceled accurately. In general, this assumption might not be valid. Corless and Leitmann [29] proposed a controller that works well for a class of nonlinear systems that has matched uncertainties which are bounded by some known continuous time functions; their proposed controller guarantees the uniform ultimate boundedness of the errors of the system.

In this section, a Corless-Leitmann-type controller is used to control the separately excited DC motor.

Definition 4.1 [29]. The error $e(t)$ is said to be uniformly ultimately bounded if there exist constants b and c, and for every $r_c \in (0, c)$, there is a constant $T = T(r_c) \geq 0$ such that

$$\|e(t_0)\| < r_c \Longrightarrow \|e(t)\| < b, \quad \forall t > t_0 + T. \tag{4.1}$$

The proposed control law is divided into a linear part and a nonlinear part. The linear part of the controller is designed using the pole placement technique. The nonlinear part of the controller is designed to resemble a Corless-Leitmann-type controller.

Let the symmetric positive definite matrix P_1 be the solution of the following Lyapunov equation:

$$A_c^T P_1 + P_1 A_c = -Q_1 \tag{4.2}$$

with $Q_1 = Q_1^T > 0$.

PROPOSITION 4.2. *The control law given by (4.3)–(4.6) when applied to the separately excited DC motor guarantees the uniform ultimate boundedness of the errors of the system:*

$$u = u_L + u_N \tag{4.3}$$

with

$$u_L = -Ke + r, \tag{4.4}$$

$$u_N = \begin{cases} -\dfrac{\mu_1}{\|\mu_1\|} \eta & \text{if } \|\mu_1\| > \epsilon, \\[2mm] -\dfrac{\mu_1}{\epsilon} \eta & \text{if } \|\mu_1\| \le \epsilon, \end{cases} \tag{4.5}$$

with

$$\mu_1 = \eta B^T P_1 e \tag{4.6}$$

and $\eta > 0$, and ϵ is a small positive scalar.

Proof. Using (2.17), (3.1), (4.3), (4.4), (2.15) and (2.18), it follows that

$$\dot{e} = A\zeta + Bf + Bu = A\zeta + Bf + B(-Ke + r + u_N) = A_c e + Bf + Bu_N. \tag{4.7}$$

Consider the following Lyapunov function candidate:

$$V_1 = e^T P_1 e. \tag{4.8}$$

Note that $V_1 > 0$ for $e \ne 0$ and $V_1 = 0$ for $e = 0$. Taking the derivative of V_1 with respect to time and using (4.7) and (4.2), it follows that

$$\begin{aligned} \dot{V}_1 &= \dot{e}^T P_1 e + e^T P_1 \dot{e} \\ &= (A_c e + Bf + Bu_N)^T P_1 e + e^T P_1 (A_c e + Bf + Bu_N) \\ &= -e^T Q e + 2e^T P_1 Bu_N + 2f^T B^T P_1 e. \end{aligned} \tag{4.9}$$

We will treat the two cases $\|\mu_1\| > \epsilon$ and $\|\mu_1\| \le \epsilon$ separately.

For the case when $\|\mu_1\| > \epsilon$ and $u_N = -(\mu_1/\|\mu_1\|)\eta$, (4.9) implies that

$$
\begin{aligned}
\dot{V}_1 &= -e^T Q e + 2 e^T P_1 B u_N + 2 f^T B^T P_1 e \\
&= -e^T Q_1 e - 2 e^T P_1 B \frac{\mu_1}{\|\mu_1\|} \eta + 2 f^T B^T P_1 e \\
&\leq -e^T Q_1 e - 2\|B^T P_1 e\| \eta + 2\|f\|^T \|B^T P_1 e\| \\
&\leq -e^T Q_1 e.
\end{aligned}
\tag{4.10}
$$

For the case when $\|\mu_1\| \leq \epsilon$ and $u_N = -(\mu_1/\epsilon)\eta$, (4.9) implies that

$$
\begin{aligned}
\dot{V}_1 &= -e^T Q_1 e + 2 e^T P_1 B u_N + 2 f^T B^T P_1 e \\
&= -e^T Q_1 e - 2 e^T P_1 B \frac{\mu_1}{\epsilon} \eta + 2 f^T B^T P_1 e \\
&\leq -e^T Q_1 e - 2\frac{\|B^T P_1 e\|^2}{\epsilon} \eta^2 + 2\|f\|^T \|B^T P_1 e\| \\
&\leq -e^T Q_1 e + 2\|B^T P_1 e\| \eta^2 \\
&\leq -e^T Q_1 e + 2\epsilon.
\end{aligned}
\tag{4.11}
$$

Therefore, it can be concluded that in both cases,

$$
\dot{V}_1 \leq -\lambda_{\min}(Q_1) \|e\|^2 + 2\epsilon,
\tag{4.12}
$$

where $\lambda_{\min}(Q_1)$ is the minimum eignevalue of Q_1. Using (4.8) and (4.12), it can be concluded that V_1 decreases monotonically along any trajectory of the closed-loop system until it reaches the compact set:

$$
\Lambda_s = \{e \mid V_1 \leq V_s\},
\tag{4.13}
$$

where V_s can be easily determined from (4.8) and (4.12).

Therefore, it can be concluded that the errors are uniformly ultimately bounded. Hence the control scheme (4.3)–(4.6) guarantees the uniform ultimate boundedness of the errors of the motor system.

The discontinuous nature of the Corless-Leitmann-type controller may be harmful to the motor. Hence, two continuous nonlinear state-feedback controllers are designed next. The controllers are similar to the Corless-Leitmann-type controller in that they work well for a class of nonlinear uncertain systems that has matched uncertainties which are bounded by some known continuous time functions. However, the main advantage of these control schemes are that they are continuous in nature.   □

5. Continuous nonlinear controllers for the DC motor

5.1. First continuous nonlinear controller for the DC motor. The control scheme is divided into a linear part and a nonlinear part. The linear control part is designed using the pole placement technique. The continuous nonlinear part of the controller is motivated by the work of [30]. The proposed controller has the advantage of guaranteeing the exponential stability of the closed-loop system.

Let the symmetric positive definite matrix P_2 be the solution of the following algebraic Riccati equation:

$$A_c^T P_2 + P_2 A_c - 2P_2 BB^T P_2 = -Q_2, \tag{5.1}$$

where $Q_2 = Q_2^T > 0$.

Define

$$\mu_2 = \eta B^T P_2 e, \quad \eta > 0, \tag{5.2}$$

also let ϵ and β be small positive scalars.

PROPOSITION 5.1. *The control law given by (5.3)–(5.6) when applied to the separately excited DC motor guarantees the exponential convergence to zero of the errors of the system:*

$$u = u_L + u_N \tag{5.3}$$

with

$$u_L = -Ke + r, \tag{5.4}$$

$$u_N = -B^T P_2 e - \phi_c, \tag{5.5}$$

$$\phi_c = \frac{\mu_2 ||\mu_2||^2}{||\mu_2||^3 + \epsilon^3 \exp(-3\beta t)} \eta. \tag{5.6}$$

Proof. Consider the following Lyapunov function candidate:

$$V_2 = e^T P_2 e. \tag{5.7}$$

Note that $V_2 > 0$ for $e \neq 0$ and $V_2 = 0$ for $e = 0$. Equation (5.7) implies that $\lambda_1 ||e||^2 \leq V_2 \leq \lambda_2 ||e||^2$, where λ_1 is the minimum eigenvalue of P_2 and λ_2 is the maximum eigenvalue of P_2.

Using (2.17), (3.1), (4.3), (4.4), (2.15), (2.18), and (5.5), it follows that

$$\dot{e}^T P_2 e = (A_c e + Bf + Bu_N)^T P_2 e = (e^T A_c^T + f^T B^T - e^T P_2 BB^T - \phi_c^T B^T) P_2 e. \tag{5.8}$$

Taking the derivative of V_2 with respect to time and using (5.8) and (5.3)–(5.6), it follows that

$$
\begin{aligned}
\dot{V}_2 &= \dot{e}^T P_2 e + e^T P_2 \dot{e} \\
&= (e^T A_c^T + f^T B^T - e^T P_2 BB^T - \phi_c^T B^T) P_2 e + e^T P_2 (A_c e + B f - BB^T P_2 e - B\phi_c) \\
&= -e^T Q_2 e + 2e^T P_2 B f - 2e^T P_2 B \phi_c^T \\
&= -e^T Q_2 e + 2e^T P_2 B f - \frac{2e^T P_2 B \mu_2 ||\mu_2||^2}{||\mu_2||^3 + \epsilon^3 \exp(-3\beta t)} \eta \\
&\le -e^T Q_2 e - \frac{2||B^T P_2 e \eta||^4}{||B^T P_2 e \eta||^3 + \epsilon^3 \exp(-3\beta t)} \eta + 2||B^T P_2 e \eta|| \\
&\le -e^T Q_2 e + \frac{2||B^T P_2 e \eta|| \epsilon^3 \exp(-3\beta t)}{||B^T P_2 e \eta||^3 + \epsilon^3 \exp(-3\beta t)} \eta \\
&\le -e^T Q_2 e + 2\epsilon \exp(-\beta t) \\
&\le -\lambda_3 ||e||^2 + 2\epsilon \exp(-\beta t).
\end{aligned}
\tag{5.9}
$$

In the above, we used the fact that

$$
0 \le \frac{ab^3}{a^3 + b^3} \le b, \quad \forall a, b \ge 0, \ a^3 + b^3 \ne 0.
\tag{5.10}
$$

and λ_3 is the minimum eigenvalue of Q_2.

Let $\kappa = \lambda_3/\lambda_2$, it follows that

$$
\dot{V}_2 \le -\kappa V_2 + 2\epsilon \exp(-\beta t).
\tag{5.11}
$$

Thus, it can be concluded that the error $e(t)$ is globally exponentially stable. Moreover, the convergence rate of the errors is such:

$$
||e(t)|| \le
\begin{cases}
\left[\dfrac{\lambda_2}{\lambda_1} ||e(0)||^2 \exp(-\kappa t) + \dfrac{2\varepsilon}{\lambda_1} t \exp(-\kappa t) \right]^{1/2} & \text{if } \beta = \kappa, \\[3ex]
\left[\dfrac{\lambda_2}{\lambda_1} ||e(0)||^2 \exp(-\kappa t) + \dfrac{2\varepsilon}{\lambda_1(\kappa - \beta)} (\exp(-\beta t) - \exp(-\kappa t)) \right]^{1/2} & \text{if } \beta \ne \kappa.
\end{cases}
\tag{5.12}
$$

Hence, it can be concluded that the proposed control scheme (5.3)–(5.6) when applied to the DC motor system guarantees the exponential convergence to zero of the errors of the system. □

5.2. Second continuous nonlinear controller for the DC motor. Again, the control scheme is divided into a linear part and a nonlinear part. The linear controller part is designed using the pole placement technique. The continuous nonlinear part of the controller is motivated by the work of [31].

Let the symmetric positive definite matrix P_3 be the solution of the Lyapunov equation:

$$A_c^T P_3 + P_3 A_c = -Q_3 \tag{5.13}$$

with $Q_3 = Q_3^T > 0$.

PROPOSITION 5.2. *The control law*

$$u = u_L + u_N \tag{5.14}$$

with

$$u_L = -Ke + r, \qquad u_N = -\gamma_o B^T P_3 e \tag{5.15}$$

when applied to the separately excited DC motor guarantees the exponential convergence of the errors of the system such that

$$\|e(t)\| \le c_o \exp\left(-\nu(t - t_o)\right) + \mu, \tag{5.16}$$

where

$$c_o = \sqrt{\frac{\lambda_{\max}(P_3)}{\lambda_{\min}(P_3)}} \|e(t_o)\|, \qquad \nu = \frac{\lambda_{\min}(Q_3)}{2\lambda_{\max}(P_3)}, \qquad \mu = \eta \sqrt{\frac{\lambda_{\max}(P_3)}{\gamma_o \lambda_{\min}(P_3)\lambda_{\min}(Q_3)}}, \tag{5.17}$$

and $\lambda_{\max}(\bullet)$ is the maximum eigenvalue of $\bullet$, and $\lambda_{\min}(\bullet)$ is the minimum eigenvalue of $\bullet$.

Proof. Consider the following Lyapunov function candidate:

$$V_3 = e^T P_3 e. \tag{5.18}$$

Note that $V_3 > 0$ for $e \neq 0$ and $V_3 = 0$ for $e = 0$.

Taking the derivative of V_3 with respect to time and using (2.17), (3.1), (2.15), and (5.11)–(5.14), it follows that

$$\begin{aligned}
\dot{V}_3 &= \dot{e}^T P_3 e + e^T P_3 \dot{e} \\
&= \left(A_c e + Bf + Bu_N\right)^T P_3 e + e^T P_3 \left(A_c e + Bf + Bu_N\right) \\
&= -e^T Q_3 e + 2e^T P_3 Bu_N + 2f^T B^T P_3 e \\
&= -e^T Q_3 e + 2e^T P_3 B\left(-\gamma_o B^T P_3 e\right) + 2f^T B^T P_3 e \\
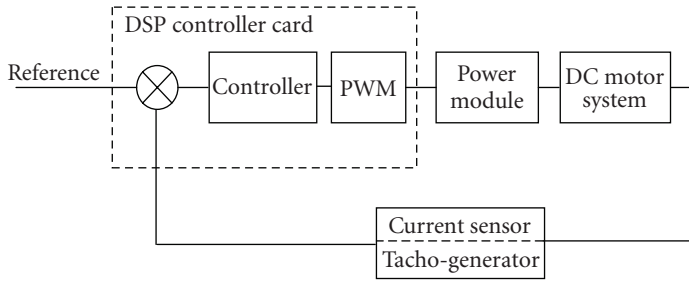&\le -e^T Q_3 e - 2\gamma_o \|B^T P_3 e\|^2 + 2\|B^T P_3 e\|\eta
\end{aligned}$$

Figure 6.1. A block diagram representation of the system.

$$= -e^T Q_3 e - 2\gamma_o \left[||B^T P_3 e||^2 - \frac{\eta}{\gamma_o} ||B^T P_3 e|| \right]$$

$$= -e^T Q_3 e - 2\gamma_o \left[||B^T P_3 e|| - \frac{\eta}{2\gamma_o} \right]^2 + \frac{\eta^2}{2\gamma_o}$$

$$\leq -e^T Q_3 e + \frac{\eta^2}{2\gamma_o}$$

$$= -\lambda_{\min}(Q_3) ||e||^2 + \frac{\eta^2}{2\gamma_o}.$$

(5.19)

Using the results of [31], it can be concluded that

$$||e(t)|| \leq c_o \exp\left(-\nu(t - t_o)\right) + \mu.$$

(5.20)

Therefore, it can be concluded that the control scheme (5.14)-(5.15) when applied to the DC motor system guarantees the exponential convergence to zero of the errors of the system with a prespecified rate of convergence and prespecified tolerance.   □

6. Description of the hardware setup

A hardware testbed was built to test the performances of the proposed control schemes. The system is composed of a DC motor system, a DSP controller board, a power module, two current sensors, and a tachogenerator. The DC motor system includes a separately excited DC motor and a DC generator which is used to simulate variable loads on the motor. A block diagram representation of the system is shown in Figure 6.1.

The derived feedback controllers are implemented using a digital signal processor (DSP) card. The algorithm for the controller is coded using the Simulink environment; then it is downloaded from the computer into the DSP which resides on a controller board. The control algorithm in the DSP, together with the other peripheral subsystems on the controller board, will ensure a smooth transition of the motor from the initial speed to the final speed under various loading conditions. A driver circuit is required to
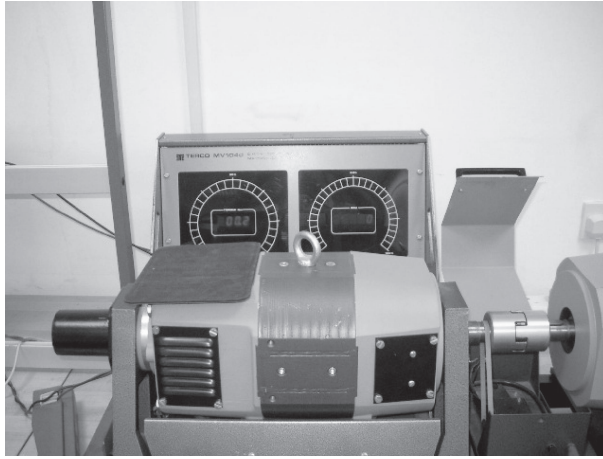
Figure 6.2. A photograph of the DC motor.

Table 6.1. Values of the parameters of the DC motor.

Parameter	Value
R_a	3.5 Ω
L_a	0.0432 H
R_f	233 Ω
L_f	25.5 H
K_m	1.9469
B_m	0.0025
J_m	0.0017

interface between the controller board and the motor; this is the case because the peripheral subsystems of the controller board have low current capabilities. Two current sensors are also used to measure the armature and field currents. A tachogenerator, from Servo-Tek, with an output of 20.8 Volt/RPM is used for speed feedback.

A separately excited permanent magnet DC motor is used to test the proposed control algorithm. A photograph of the DC motor is shown in Figure 6.2. The motor (an MV1042-225 motor) has the specifications shown in Tables 6.1 and 6.2.

In order to study the performance of the system under different loading conditions, the motor shaft is coupled with a DC generator. The output of the DC generator is then connected to an adjustable resistive load. A switching arrangement is made to provide a step change in the load.

The nonlinear region of operation for a DC motor starts above the base speed. A decrease in field voltage v_f (which, in turn, reduces the field current i_f) increases the motor speed. To implement such a system, a buck converter is used. The first step is to rectify

Table 6.2. Ratings of the DC motor.

Parameter	Rating
Rated armature voltage	220 Volt
Rated field voltage	220 Volt
Rated power	3 KW
Rated speed	1400 RPM

the AC voltage and to filter out the voltage ripple. The AC-to-DC converter is implemented using a bridge rectifier along with an LC filter. A DC-to-DC chopper is then used to obtain varying field voltages. Pulse width modulation (PWM) is used with a switching frequency of 5 KHz. In addition, IGBTs are used as power switches and compatible high-speed switching diodes to "free wheel" the current during the energy release phase. The heart of the driver circuitry is an IR2125 chip capable of providing high switching current along with overcurrent protection. A high-speed optoisolator is also used to connect the driver chip to the control board. Such an arrangement is needed to provide ground isolation and to reduce signal noise.

A real-time interface (RTI) board (the DS1104 Board) is used to program the control algorithm. This board is manufactured by the dSPACE Company. The software language used to program the DSP board is Simulink. This tool is a quite powerful combination of graphic user interface (GUI), in the MATLAB environment, and the digital signal processor board with a built-in data acquisition system. The PWM slave module of the controller greatly simplified the hardware implementation. A high-speed analog-to-digital converter (ADC) made it possible to implement the derived continuous design in the available digital environment.

7. Implementation results

The developed control schemes are implemented using the hardware setup described in the previous section.

The DC motor is commanded to speed up from an initial angular velocity of 1500 rpm to a final speed of 2500 rpm. Note that the rated speed of the motor is 1400 rpm; the motor is therefore commanded to operate *above* the rated speed. The gains of the controllers are

$$K_1 = \begin{bmatrix} 1029 & -29 & 0 \\ 0 & 0 & 91 \end{bmatrix}, \qquad K_2 = \begin{bmatrix} 2398 & 8.5 & 0 \\ 0 & 0 & 1 \end{bmatrix}. \tag{7.1}$$

The feedback linearization controller given by (3.2) is implemented first. The gain $K = K_1$ was used. The implementation results are shown in Figures 7.1–7.3. Figure 7.1 shows the speed versus time profile. Figure 7.2 and Figure 7.3 show the field current and the armature currents, respectively. It is clear from the figures that the motor is regulated to the desired speed in a very short period of time. However, the speed profile of the motor exhibits a small steady-state error.
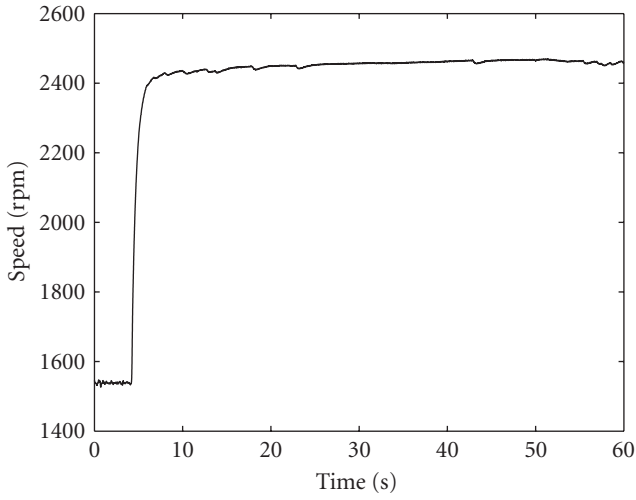
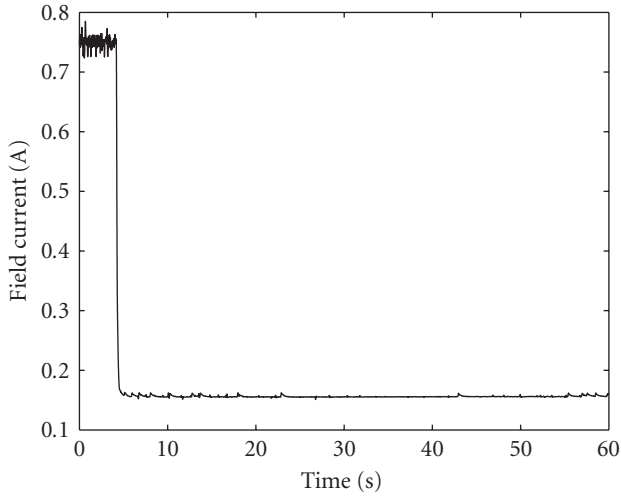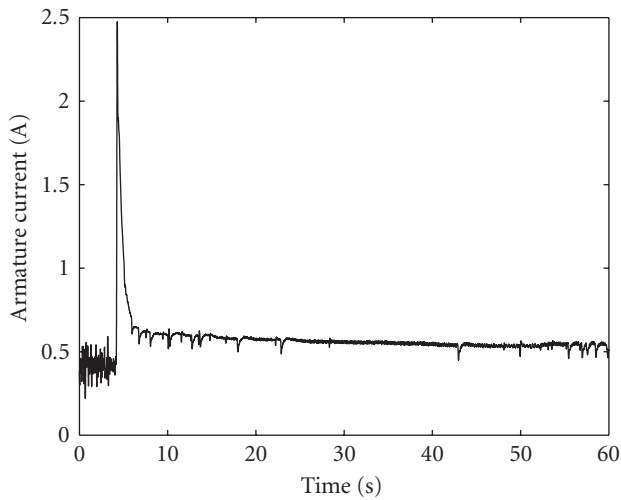Figure 7.1. Speed ω when the feedback linearization controller is used.

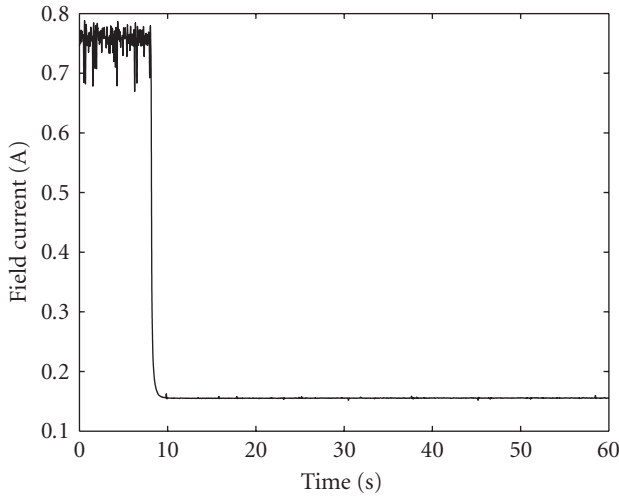Figure 7.2. Field current i_f when the feedback linearization controller is used.

The implementation results when the Corless-Leitmann-type controller given by (4.3)–(4.6) is used are shown in Figures 7.4–7.6. The gain $K = K_2$ was used. Figure 7.4 shows the speed versus time profile. Figure 7.5 and Figure 7.6 show the field current and the armature currents, respectively. It is clear from the figures that the motor is regulated to the desired speed in a very short period of time.

Figure 7.3. Armature current i_a when the feedback linearization controller is used.
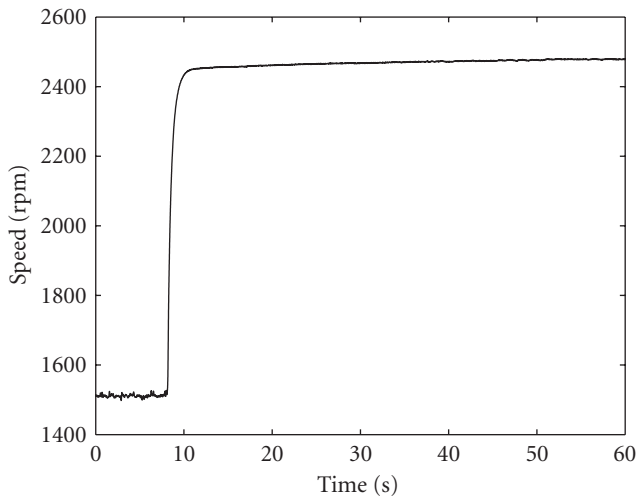
Figure 7.4. Speed ω when the Corless-Leitmann-type controller is used.

The implementation results when the first continuous nonlinear controller given by (5.3)–(5.6) is used are shown in Figures 7.7–7.9. The gain $K = K_1$ was used. Figure 7.7 shows the speed versus time profile. Figure 7.8 and Figure 7.9 show the field current and the armature currents, respectively. It is clear from the figures that the motor is regulated to the desired speed in a very short period of time. However, the speed profile of the

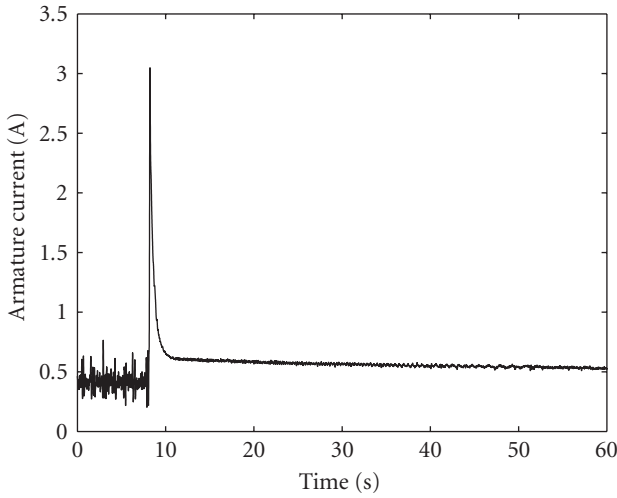Figure 7.5. Field current i_f when the Corless-Leitmann-type controller is used.

Figure 7.6. Armature current i_a when the Corless-Leitmann-type controller is used.

motor exhibits some chattering around the desired speed. This chattering is due to the ϕ_c term given in (5.6).

   The implementation results when the second continuous nonlinear controller given by (5.14)-(5.15) is used are shown in Figures 7.10–7.12. The gain $K = K_1$ was used. Figure 7.10 shows the speed versus time profile. Figure 7.11 and Figure 7.12 show the
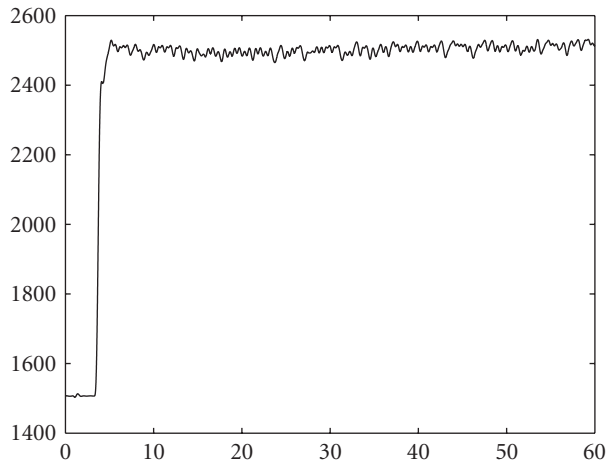
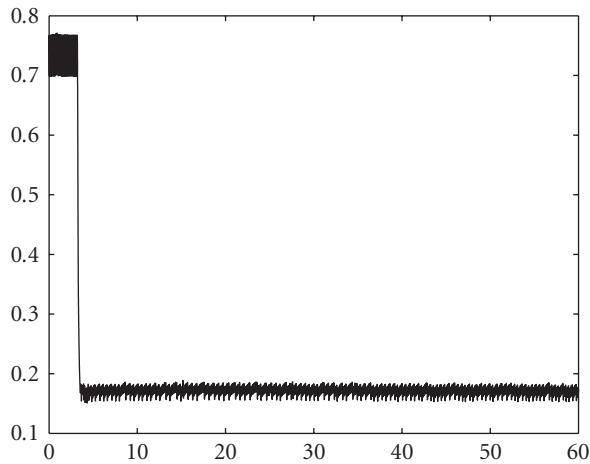Figure 7.7. Speed ω when the first continuous nonlinear controller is used.

Figure 7.8. Field current i_f when the first continuous nonlinear controller is used.

field current and the armature currents, respectively. It is clear from the figures that the motor is regulated to the desired speed in a very short period of time.

Comparing the performances of the four proposed controllers, it can be concluded that the second continuous nonlinear controller given by (5.14)-(5.15) gave the best performance; the Corless-Leitmann-type controller gave the second best performance.

Moreover, it is found that the amplitudes of the control signals for the four different control schemes are within acceptable ranges. It should be noted that a DC-to-DC chopper is used to obtain varying field voltages, and pulse width modulation (PWM) is used with a switching frequency of 5 KHz.
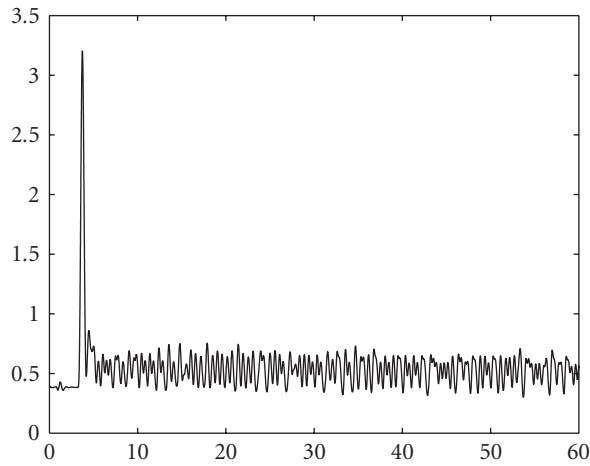
Figure 7.9. Armature current i_a when the first continuous nonlinear controller is used.
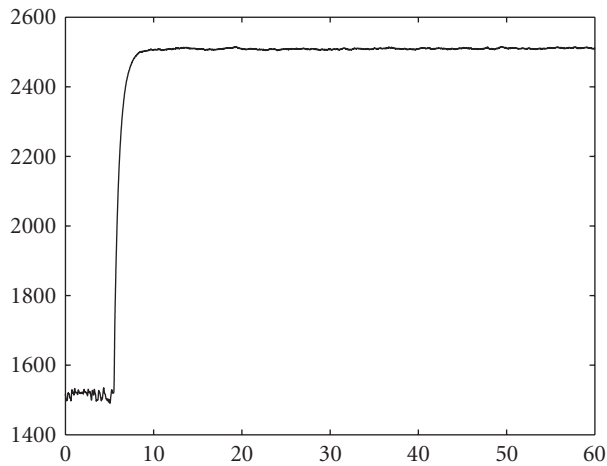

Figure 7.10. Speed ω when the second continuous nonlinear controller is used.

Also, the robustness of the proposed controllers with respect to changes in the load attached to the motor is tested. Experimental tests indicate that the feedback linearization controller is not robust to changes in the load. However, the Corless-Leitmann controller as well as the other two controllers are found to be robust to changes in the load attached to the motor.

8. Conclusion

The problem of controlling a separately excited DC motor operating in the field-weakening region using nonlinear controllers is studied in this paper. A feedback linearization
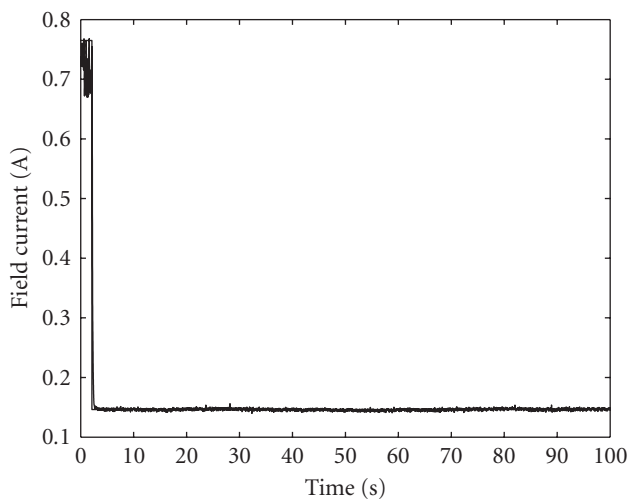
Figure 7.11. Field current i_f when the second continuous nonlinear controller is used.
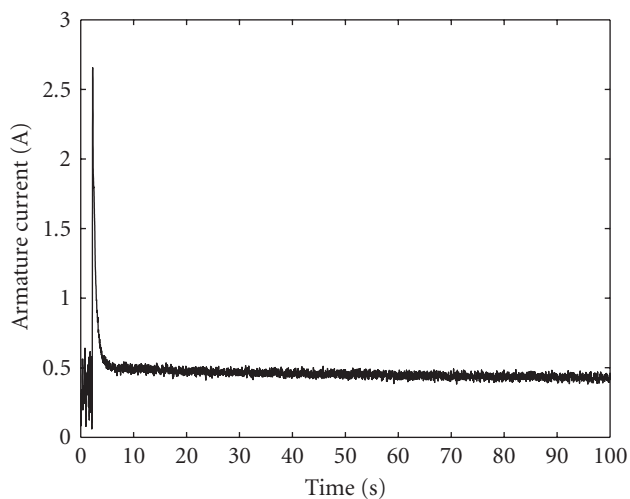

Figure 7.12. Armature current i_a when the second continuous nonlinear controller is used.

controller, a Corless-Leitmann-type controller and two continuous nonlinear controllers are designed for the system. Implementation results of the proposed control schemes show that the proposed controllers work well.

Robustness of the proposed control schemes to changes in the load and to changes in the parameters of the system will be the topic of future research. Design and implementation of sliding mode controllers will be another topic of future research.

Acknowledgment

References

[1] M. Bodson and J. Chiasson, "Differential-geometric methods for control of electric motors," *International Journal of Robust and Nonlinear Control*, vol. 8, no. 11, pp. 923–954, 1998.

[2] M. Bodson, J. Chiasson, and R. Novotnak, "High-performance induction motor control via input-output linearization," *IEEE Control Systems Magazine*, vol. 14, no. 4, pp. 25–33, 1994.

[3] T. C. Burg, D. M. Dawson, J. Hu, and P. Vedagarbha, "Velocity tracking control for a separately excited DC motor without velocity measurements," in *Proceedings of the American Control Conference*, vol. 1, pp. 1051–1056, Baltimore, Md, USA, June-July 1994.

[4] J. Chiasson, "Nonlinear differential-geometric techniques for control of a series DC motor," *IEEE Transactions on Control Systems Technology*, vol. 2, no. 1, pp. 35–42, 1994.

[5] J. Chiasson and M. Bodson, "Nonlinear control of a shunt DC motor," *IEEE Transactions on Automatic Control*, vol. 38, no. 11, pp. 1662–1666, 1993.

[6] R. Harmsen and J. Jiang, "Control of a separately excited DC motor using on-line linearization," in *Proceedings of the American Control Conference*, vol. 2, pp. 1879–1883, Baltimore, Md, USA, June-July 1994.

[7] M. H. Nehrir and F. Fatehi, "Tracking control of DC motors via input-output linearization," *Electric Machines and Power Systems*, vol. 24, no. 3, pp. 237–247, 1996.

[8] P. D. Olivier, "Feedback linearization of DC motors," *IEEE Transactions on Industrial Electronics*, vol. 38, no. 6, pp. 498–501, 1991.

[9] D. G. Taylor, "Nonlinear control of electric machines: an overview," *IEEE Control Systems Magazine*, vol. 14, no. 6, pp. 41–51, 1994.

[10] V. I. Utkin, "Sliding mode control design principles and applications to electric drives," *IEEE Transactions on Industrial Electronics*, vol. 40, no. 1, pp. 23–36, 1993.

[11] F. Briz, A. Diez, M. W. Degner, and R. D. Lorenz, "Current and flux regulation in field-weakening operation [of induction motors] ," *IEEE Transactions on Industry Applications*, vol. 37, no. 1, pp. 42–50, 2001.

[12] A. Buente, H. Grotstollen, and P. Krafka, "Field weakening of induction motors in a very wide region with regard to parameter uncertainties," in *Proceedings of the 27th Annual IEEE Power Electronics Specialists Conference (PESC '96)*, vol. 1, pp. 944–950, Maggiore, Italy, January 1996.

[13] K. Sattler, U. Schaefer, and R. Gheysens, "Field oriented control of an induction motor with field weakening under consideration of saturation and rotor heating," in *Proceedings of the 4th International Conference on Power Electronics and Variable-Speed Drives*, pp. 286–291, London, UK, July 1990.

[14] B. J. Seibel, T. M. Rowan, and R. J. Kerkman, "Field-oriented control of an induction machine in the field-weakening region with DC-link and load disturbance rejection," *IEEE Transactions on Industry Applications*, vol. 33, no. 6, pp. 1578–1584, 1997.

[15] R. Krishnan, "Control and operation of PM synchronous motor drives in the field-weakening region," in *Proceedings of the 19th International Conference on Industrial Electronics, Control and Instrumentation (IECON '93)*, vol. 2, pp. 745–750, Maui, Hawaii, USA, November 1993.

[16] S. Nishikata, W. Takanami, T. Kataoka, and A. Ishizaki, "Consideration to the operation limit of a field-weakening speed control system for a self-controlled synchronous motor," in *Proceedings of the 5th European Conference on Power Electronics and Applications*, vol. 5, pp. 354–359, Brighton, UK, September 1993.

[17] Z. Z. Liu and F. L. Luo, "Nonlinear multi-input multi-output control of DC motor in fieldweakening region," in *Proceedings of International Conference Electric Machines and Drives (IEMD '99)*, pp. 688–690, Seattle, Wash, USA, May 1999.

[18] Z. Z. Liu, F. L. Luo, and M. H. Rashid, "Nonlinear load-adaptive MIMO controller for high performance DC motor field weakening," in *IEEE Power Engineering Society Winter Meeting*, vol. 1, pp. 332–337, Singapore, January 2000.

[19] Z. Z. Liu, F. L. Luo, and M. H. Rashid, "Speed nonlinear control of DC motor drive with field weakening," *IEEE Transactions on Industry Applications*, vol. 39, no. 2, pp. 417–423, 2003.

[20] F. L. Luo, Z. Z. Liu, and D. Tien, "Nonlinear field weakening controller of a separately excited DC motor," in *Proceedings of the International Conference on Energy Management and Power Delivery (EMPD '98)*, vol. 2, pp. 552–557, Singapore, March 1998.

[21] M. R. Matausek, B. I. Jeftenic, D. M. Miljkovic, and M. Z. Bebic, "Gain scheduling control of DC motor drive with field weakening," *IEEE Transactions on Industrial Electronics*, vol. 43, no. 1, pp. 153–162, 1996.

[22] M. R. Matausek, D. M. Miljkovic, and B. I. Jeftenic, "Nonlinear multi-input-multi-output neural network control of DC motor drive with field weakening," *IEEE Transactions on Industrial Electronics*, vol. 45, no. 1, pp. 185–187, 1998.

[23] J. Zhou, Y. Wang, and R. Zhou, "Adaptive backstepping control of separately excited DC motor with uncertainties," in *Proceedings of International Conference on Power System Technology (PowerCon '00)*, vol. 1, pp. 91–96, Perth, Western Australia, August 2000.

[24] J. Zhou, Y. Wang, and R. Zhou, "Global speed control of separately excited DC motor," in *Proceedings of the IEEE Power Engineering Society Winter Meeting*, vol. 3, pp. 1425–1430, Columbus, Ohio, USA, January-February 2001.

[25] G. K. Miti and A. C. Renfrew, "Analysis, simulation and microprocessor implementation of a current profiling scheme for field-weakening applications and torque ripple control in brushless DC motors," in *Proceedings of the 9th International Conference on Electrical Machines and Drives (EMD '99)*, pp. 361–365, Canterbury, UK, September 1999.

[26] G. K. Miti, A. C. Renfrew, and B. J. Chalmers, "Field-weakening regime for brushless DC motors based on instantaneous power theory," *IEE Proceedings: Electric Power Applications*, vol. 148, no. 3, pp. 265–271, 2001.

[27] H. Zeroug, D. Holliday, D. Grant, and N. Dahnoun, "Performance prediction and field weakening simulation of a brushless DC motor," in *Proceedings of the 8th International Conference on Power Electronics and Variable Speed Drives*, pp. 321–326, London, UK, September 2000.

[28] M. Zribi and J. Chiasson, "Position control of a PM stepper motor by exact linearization," *IEEE Transactions on Automatic Control*, vol. 36, no. 5, pp. 620–625, 1991.

[29] M. J. Corless and G. Leitmann, "Continuous state feedback guaranteeing uniform ultimate boundedness for uncertain dynamic systems," *IEEE Transactions on Automatic Control*, vol. 26, no. 5, pp. 1139–1144, 1981.

[30] S. K. Nguang and M. Fu, "Global quadratic stabilization of a class of nonlinear systems," *International Journal of Robust and Nonlinear Control*, vol. 8, no. 6, pp. 483–497, 1998.

[31] S. Zenieh and M. Corless, "Simple robust r-α tracking controllers for uncertain fully-actuated mechanical systems," *Transactions of the ASME, Journal of Dynamic Systems, Measurement and Control*, vol. 119, no. 4, pp. 821–825, 1997.

Mohamed Zribi: Department of Electrical Engineering, Kuwait University, P.O. Box 5969, Safat 13060, Kuwait
Email address: mzribi@eng.kuniv.edu.kw

Adel Al-Zamel: Department of Electrical Engineering, Kuwait University, P.O. Box 5969, Safat 13060, Kuwait
Email address: alzamel@eng.kuniv.edu.kw